

Enhanced cross-flow filtration with flat-sheet ceramic membranes by titanium-based coagulation for membrane fouling control

Xiaoman Liu¹, Chang Tian², Yanxia Zhao (✉)¹, Weiyang Xu¹, Dehua Dong³, Kaimin Shih⁴, Tao Yan¹, Wen Song¹

¹ School of Water Conservancy and Environment, University of Jinan, Jinan 250022, China

² School of Environmental Science and Engineering, Qilu University of Technology (Shandong Academy of Sciences), Jinan 250353, China

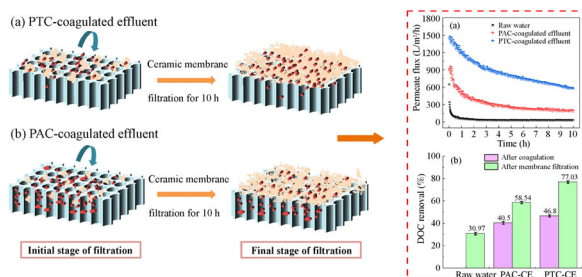
³ School of Material Science and Engineering, University of Jinan, Jinan 250022, China

⁴ Department of Civil Engineering, The University of Hong Kong, Hong Kong 999077, China

HIGHLIGHTS

- Ceramic membrane filtration showed high performance for surface water treatment.
- PTC pre-coagulation could enhance ceramic membrane filtration performance.
- Ceramic membrane fouling was investigated by four varied mathematical models.
- PTC pre-coagulation was high-effective for ceramic membrane fouling control.

GRAPHIC ABSTRACT



ARTICLE INFO

Article history:

Received 18 June 2021

Revised 3 November 2021

Accepted 22 November 2021

Available online 6 January 2022

Keywords:

Ceramic membrane
Coagulation
Polytitanium chloride
Membrane fouling

ABSTRACT

Application of ceramic membrane (CM) with outstanding characteristics, such as high flux and chemical-resistance, is inevitably restricted by membrane fouling. Coagulation was an economical and effective technology for membrane fouling control. This study investigated the filtration performance of ceramic membrane enhanced by the emerging titanium-based coagulant (polytitanium chloride, PTC). Particular attention was paid to the simulation of ceramic membrane fouling using four widely used mathematical models. Results show that filtration of the PTC-coagulated effluent using flat-sheet ceramic membrane achieved the removal of organic matter up to 78.0%. Permeate flux of ceramic membrane filtration reached 600 L/(m²·h), which was 10-fold higher than that observed with conventional polyaluminum chloride (PAC) case. For PTC, fouling of the ceramic membrane was attributed to the formation of cake layer, whereas for PAC, standard filtration/intermediate filtration (blocking of membrane pores) was also a key fouling mechanism. To sum up, cross-flow filtration with flat-sheet ceramic membranes could be significantly enhanced by titanium-based coagulation to produce both high-quality filtrate and high-permeation flux.

© Higher Education Press 2022

1 Introduction

Membrane technology is a water treatment technology that effectively removes suspended particles, colloids, and organic pollutants from polluted water (Werber et al., 2016). Ceramic membrane is becoming increasingly attractive due to their unique advantages, which include

heat resistance, corrosion resistance, resistance against biological pollution and long service life (Wei et al., 2021). These advantages enable ceramic membranes to be widely used in the treatment of surface water, municipal wastewater, and drinking water (Li et al., 2020).

Membrane fouling is a critical issue, especially during the pressure-driven process of wastewater filtration. Coagulation is regarded as one of the most successful pretreatment technologies against membrane fouling due to its low cost, high performance, and the ability to remove natural organic matters (Zhang et al., 2022). The most

✉ Corresponding author

E-mail: Stu_zhaoyx@ujn.edu.cn

widespread coagulants are Al- and Fe-based salts owing to superior coagulation performance and cost-efficiency (Zhao et al., 2014; Chekli et al., 2017). Although, there are problems of biological toxicity and effluent coloring respectively existing in the coagulation process applying Al- and Fe-based salts. By contrast, titanium-based coagulants have attracted wide attention in recent years due to innocuity, excellent performance and sludge recycling (Shon et al., 2010). Using titanium-based coagulants instead of Al- and Fe-based coagulants could achieve high-efficient water purification and sludge recycling goals. Pre-coagulation using titanium-based coagulants before ceramic membrane filtration could be an efficient strategy against membrane fouling and water quality improvement. Considering these aspects, the Ti-based pre-coagulation followed by ceramic membrane filtration could result in 1) high-quality filtrate, 2) mitigated membrane fouling, and 3) recyclable primary sludge.

The characterization of the mechanism associated with ceramic membrane fouling has been attracting a lot of attention. Researchers have conducted extensive research and characterization on membrane fouling mechanism based on organic membrane (OM) filtration, such as the filtration resistance-in-series model (Xu et al., 2016), the combined pore blockage-cake filtration model (Hou et al., 2017), and comprehensive membrane fouling index (MFI) model (Zhan et al., 2021), etc. Only a few studies on ceramic membrane fouling have been reported. Li et al. studied membrane fouling in the process of sugarcane juice filtration with ceramic membrane, adopting the comprehensive analysis method of fouling resistance model, continuous fouling model, scanning electron microscope (SEM), and atomic force microscope (AFM) (Li et al., 2019). Ma et al. found that the pollution mechanism changed from pore blocking to cake formation at a particular time when self-made ceramic membrane was used to filter humic acid solution and surface water (Ma et al., 2010). Fouling mechanism of ceramic membrane is complicated and not dominated by a single pollution mechanism. The mechanism and degree pollution differ with different feeding solutions. For the actual water samples with complex components, it is more reasonable and reliable to combine different models to analyze membrane fouling in membrane filtration process. In this study, for the hybrid process of titanium-based pre-coagulation and ceramic membrane filtration, investigation of the ceramic membrane fouling mechanisms will provide theoretical support for the membrane fouling control during practical application process of this technology.

This study investigated the cross-flow filtration with flat-sheet ceramic membranes for lake water purification. Pre-coagulation with PTC was utilized to enhance the filtration performance. Furthermore, pre-coagulation with conventional polyaluminum chloride was assessed for comparison. Coagulation performance was evaluated in terms of both turbidity and organic matter removal, while the

performance of the ceramic membrane filtration was characterized in terms of both filtrate flux and filtrate quality. Special efforts were paid to investigate the ceramic membrane fouling using the Hermia's model and other mathematical models.

2 Materials and methods

2.1 Membranes, coagulants, and test water

Flat-sheet Al₂O₃ ceramic membranes (100 nm, Zhongqing environmental technology, China) and polyvinylidene fluoride (PVDF) membranes (220 nm, Mosu, China) were utilized as membrane materials for filtration unit.

PTC and PAC were prepared by slow titration methodology according to our previous studies (Zhao et al., 2017). In detail, TiCl₄ solution (20%) was prepared by slowly adding TiCl₄ (99% purity) into deionized water under continuous magnetic stirring. Certain amounts of NaOH and Na₂CO₃ solution were titrated into TiCl₄ (20 wt%) and AlCl₃ solution, respectively. The basicity of PTC and PAC was calculated as molar ratio of [OH]/[Ti] and [OH]/[Al], respectively. The highest coagulation was achieved at a basicity of 1.5, and hence, this value was selected for both PTC and PAC in this study. The concentrations of PTC and PAC are expressed as mg Ti/L and mg Al/L, respectively. All reagents (analytical purity grade) were purchased from Aladdin Biochemical Technology (China) without further purification.

Test water was obtained from Jiazi Lake at University of Jinan, Shandong Province, China. The water quality parameters were as follows: residual turbidity = 3.04±0.67 NTU, UV₂₅₄ = 0.11±0.002 cm⁻¹, dissolved organic carbon (DOC) = 14.57±1.01 mg/L, Zeta potential = -14.38±0.55 mV, pH = 8.72±0.04.

2.2 Jar-test

Coagulation tests were operated on a program-controlled jar-tester (MY 3000-6M, Wuhan Meiyu, China). A predetermined amount of PTC or PAC was added to the test water and stirred continuously for 1.5 min at a stir speed of 200 r/min (velocity gradient, G of 250 s⁻¹). After that, the speed of the agitator was adjusted to 40 r/min (G of 22.3 s⁻¹) for 15 min, followed by sedimentation for 30 min. Finally, the supernatant was drawn from 2 cm around below the solution surface for water quality assessment.

The turbidity of water samples was determined by 2100Q turbidimeter (Hach, USA). The test water was filtered with 0.45 μm cellulose acetate membrane, and the measurement of DOC and the ultraviolet absorbance at 254 nm (UV₂₅₄) was carried out on TOC-L CPH CN200 analyzer (Shimadzu, Japan) and TU-1810PC ultraviolet spectrophotometer (Purkinje General Instrument, China), respectively. Using a Fluoromax-4 fluorescence spectrophotometer (Santec,

Japan), three-dimensional fluorescence excitation emission matrix spectra was applied to determine dissolved organic matter. It was scanned over excitation (Ex) wavelengths of 220–500 nm at an interval of 5 nm and emission (Em) wavelengths of 250–550 nm at an interval of 5 nm. The pH of the solution was measured by pHS-3C pH meter (INESA Scientific Instrument, China). Zeta potential was analyzed using Malvern Zetasizer Nano-ZS90 (Malvern Instrument, Germany). Particle size distribution (PSD) was determined by using a Mastersizer 3000 laser particle size analyzer (Mastersizer, UK).

2.3 Cross-flow filtration with ceramic membrane

The filtration experiments with ceramic membrane were carried out on a cross-flow filtration device as shown in Fig. S1. The membrane module was equipped with one piece of flat ceramic membrane, with the effective filtration area of 18 cm² (6 cm Length × 3 cm Width). To understand the effect of coagulation pretreatment on membrane filtration performance, the raw water (RW) obtained from Jiazi Lake and supernatant coagulation by PTC/PAC following with settling down for 30 min were utilized as feeding water, respectively. The feeding water was pumped into the membrane module at a constant pressure of 30 kPa by a high-pressure circulating pump with a constant pump speed of 1000 r/min. One part of the feeding water flowed back to the feeding tank from the upper direction parallel to the membrane surface, while the other part of the feeding water permeated through the ceramic membrane and flowed down into the filtrate tank through the hollow part of the ceramic membrane. The quantity of the permeate was determined on-line by an electronic balance connected to a computer for data recording. The performance of filtration with the PVDF membrane was conducted for comparison. The surface morphology of the pristine membrane and fouled membrane was characterized by a Gemini 300 field emission scanning electron microscope (Zeiss, Germany).

2.4 Characterization of ceramic membrane fouling

Four commonly used mathematical models were utilized to characterize the fouling of ceramic membranes as shown in Table 1. In detail, model 1 represents the normalized flux (J/J_0) generally applicable to any filtration mode and its changing trend vs. filtration period to represent the fouling degree of the membrane, where J is the permeate flux (L/(m²·h)) and J_0 is the initial permeate flux (L/(m²·h)).

Model 2, which was developed by Hermia, reveals the mechanism of membrane fouling in dead-end filtration under constant pressure. Due to the limitation of available models, this model is also commonly utilized to fit flux decline data in cross-flow filtration (He and Vidic, 2016). The equation is calculated as follows (Eq. (1)) (Wang et al., 2017; Yang et al., 2019):

$$\frac{d^2t}{dV^2} = k \left(\frac{dt}{dV} \right)^n, \quad (1)$$

where t is the filtration time (s), V is the total permeate volume (m³), k is the fouling coefficient and n is the filtration constant. The values of n were obtained from the fitting of d^2t/dV^2 and dt/dV (Ghalami Chooabar et al., 2019). Then values of 0, 1, 1.5 and 2, represent cake filtration, intermediate blocking, standard blocking, and complete blocking, respectively (Table 1). The d^2t/dV^2 and dt/dV can also be expressed by flux, calculated as follows (Eqs. (2) and (3)):

$$\frac{dt}{dV} = \frac{1}{JA}, \quad (2)$$

$$\frac{d^2t}{dV^2} = -\frac{1}{J^3A^2} \frac{dJ}{dt}, \quad (3)$$

where J is the permeate flux (L/(m²·h)) and A is the membrane area (m²). dJ/dt is obtained by nonlinear fitting of flux and time.

Simultaneously, the standard law filtration and classical cake filtration model which were reported by Visvanathan and Ben aim to explain the retention mechanism of colloidal particles on membrane surface and in membrane pores in cross-flow filtration constant pressure were used to characterize membrane fouling (Visvanathan and Ben aim, 1989; Zhao and Li, 2019). The formula of the standard law filtration mode and classical cake filtration are shown in model 3 in Table 1. The fitting curves of $t/V-V$ and $t/V-T$ represent the standard law filtration and classical cake filtration model, respectively. The mechanism of membrane fouling in the process of membrane filtration is determined by analyzing the fitting degree of the fitting curve.

To analyze the dissimilarity of membrane fouling mechanism between the fast flux decline stage and the slow flux decline stage in the late filtration stage, the linear expression of Hermia's model was employed to evaluate the decrease in membrane flux under constant pressure mode (model 4, Table 1) (Jia et al., 2019). This model is capable of universal applicability to constant pressure and constant current modes in low pressure membrane filtration (Huang et al., 2008; Shen et al., 2010). The correlation coefficient (R^2) of the fitting curve ($1/J-V$, $\ln J-V$, $J^{1/2}-V$, and $J-V$) was utilized as the evaluation index. The higher the R^2 value means that the corresponding membrane fouling mechanism plays a major role in the membrane filtration process.

3 Results and discussion

3.1 Performance of coagulation with PTC

The performance of coagulation with PTC for water purification was investigated in terms of both turbidity,

Table 1 Four membrane filtration models for characterizing ceramic membrane fouling

Models	Calculation formulas	Evaluation parameter	Parameter characterization for membrane fouling mechanism	Nomenclature	References
Model 1	J/J_0-t	J/J_0	The value of J/J_0 represents the degree of membrane fouling. The decreasing trend of J/J_0 indicates developing rate of membrane fouling.	J : permeate flux ($L/(m^2 \cdot h)$); J_0 : initial permeate flux ($L/(m^2 \cdot h)$); t : filtration time (h)	He and Vidić, 2016; Park et al., 2019
Model 2	$\frac{d^2t}{dV^2} = a \left(\frac{dt}{dV} \right)^n, \quad (4)$	n	$n = 0$, cake filtration (the particles cannot enter the membrane pores and accumulate on the membrane surface to form a permeable cake layer); $n = 1$, intermediate blocking (the particles settle on previously deposited dirt particles or the unobstructed area of the membrane, similar to complete blockage); $n = 1.5$, standard blocking (the particles enter and adsorb in the membrane pores, reducing the pore size); $n = 2$, complete blocking (the particle size is larger than the membrane pore so that it cannot enter the membrane pore and deposit on the membrane surface to block the pore entrance)	t : filtration time (s); V : accumulated filtration volume (m^3); J : permeate flux ($L/(m^2 \cdot h)$); A : effective filtration area (m^2); n : the filtration constant characterizing the filtration mechanism; a : fouling coefficient	Wang et al., 2017; Yang et al., 2019
	$\frac{dt}{dV} = \frac{1}{JA}, \quad (5)$				
	$\frac{d^2t}{dV^2} = -\frac{1}{J^2 A^2} \frac{dJ}{dt}, \quad (6)$				
Model 3	$\frac{t}{V} = \frac{1}{Q_0} + \frac{b_1 t}{2}, \quad (7)$	R^2	Curve 1: $t/V-t$, standard law filtration (deposit of particles smaller than the membrane pore size onto the pore walls, reducing the pore size); Curve 2: $t/V-V$, cake filtration (deposit of particles larger than the membrane pore size onto the membrane surface.) The higher R^2 , the more likely the membrane fouling mechanism represented by the fitting line	t : filtration time (s); V : accumulated filtration volume (m^3); V_f : permeate volume (m^3); Q_0 : initial flux rate (L/h); b_1, b_2 : filtration constant	Viswanathan and Ben aim, 1989; Zhao and Li, 2019
	$\frac{t}{V} = \frac{1}{Q_0} + \frac{b_2 V}{2}, \quad (9)$				
Model 4	$\frac{1}{J'} = 1 + k_1 V, \quad (10)$	R^2	$1/J'-V$, cake filtration (same as model 2); $\ln J'-V$, intermediate blocking (same as model 2); $J'^{1/2}-V$, standard blocking (same as model 2); $J'-V$, complete blocking (same as model 2) The higher R^2 , the more likely the membrane fouling mechanism represented by the fitting line	J' : the normalized flux, ration of J to J_0 ; V : accumulated filtration volume (m^3); k_1, k_2, k_3, k_4 : fouling coefficient	Huang et al., 2008; Shen et al., 2010; Jia et al., 2019
	$\ln J' = -k_2 V, \quad (11)$				
	$J'^{\frac{1}{2}} = 1 - \frac{k_3 V}{2}, \quad (12)$				
	$J' = 1 - k_4 V, \quad (13)$				

organic matter removal, zeta potential and pH (Fig. 1). Coagulation with conventional PAC was herein for comparison.

Within the dosages of coagulant investigated, residual turbidity after PAC coagulation only showed small fluctuations (0.8–1.2 NTU). By contrast, PTC dosage significantly influenced residual turbidity, with the results showing its sharp decrease from around 3.2 to 0.8 NTU with increasing PTC dosage from 15 to 40 mg Ti/L (Fig. 1(a)). Additionally, unlike PAC, PTC coagulation resulted into the effluent with lower pH value, especially at the optimized dosage condition. At 50 mg Ti/L, an effluent with a pH of about 4.0 was produced. According to our previous study (Zhao et al., 2013), the use of flocculant aid

could compensate for this disadvantage. These disadvantages could not hinder the application prospects of PTC coagulation due to its high ability to remove organic matter.

As shown in Figs. 1(b) and 1(c), a significant advantage of PTC over PAC, with regard to the removal of organic matter, was observed. PTC coagulation achieved UV_{254} removal up to 65.7% (50 mg/L), which was around 20% higher than PAC coagulation (about 46.8%, 40 mg/L). Moreover, PTC showed higher DOC removal (about 10%) than PAC. Regardless of PTC or PAC, both UV_{254} and DOC removal efficiency increased with increasing coagulant dosage. The highest removal of organic matter with the least coagulant dosage was our criteria to select the

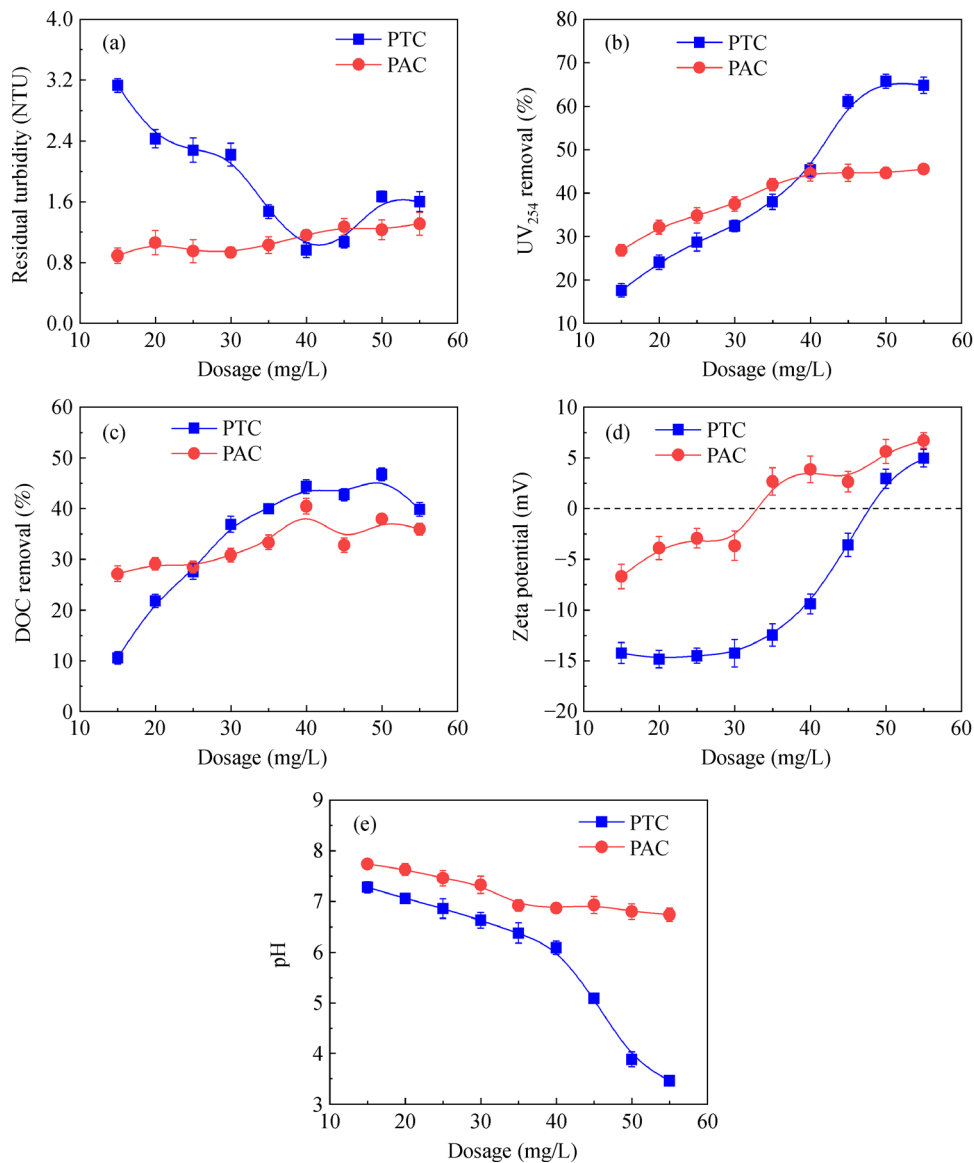


Fig. 1 Performance of coagulation with polytitanium chloride (PTC) and polyaluminum chloride (PAC): (a) residual turbidity; (b) UV_{254} removal; (c) removal of dissolved organic carbon (DOC); (d) zeta potential of coagulated flocs; (e) effluent pH after coagulation.

optimum coagulant dosage. In this study, dosage of 40 mg/L was the optimum option for PAC as the highest removal of DOC and UV₂₅₄. Whilst, in PTC case, the removal of DOC was almost the same within the PTC dosage of 35–50 mg/L. Selection of PTC dosage of 50 mg/L as the optimized one was attributed to the highest UV₂₅₄ removal up to 65.7%.

The three-dimensional fluorescence spectrum (3DEEM) was utilized to gain a further understanding the species of organic matter in PTC/PAC-coagulated effluent. Figure 2 exhibits the most fluorescent response detected at an intense peak (Ex/Em = 325–390 nm/390–475 nm) in the region V, which meant that humic-like substances occupy a dominant position in the RW (division of fluorescence spectral regions detailed in Table S1). After coagulation, the fluorescence intensity at the characteristic peak of the effluent of PTC and PAC was weakened in varying degrees, following the fluorescence intensity order of PTC < PAC. Compared with PAC, PTC removed humic-like substances belonging to the region (Ex/Em = 340–375 nm/420–460 nm) to a lower level. This indicated that PTC was more effective in the removal of humic acid at the optimal dosage.

Clarifying the mechanism of PTC coagulation will provide valuable reference for its future practical application. Changes in zeta potential of the coagulated flocs

during coagulation process was a pervasive method to characterize the coagulation mechanism (Galloux et al., 2015). Figure 1(d) shows the variation of floc zeta potential vs. coagulant dosage, with the results showing its gradual increase with increasing dosage. Coagulant dosage has always been an important factor affecting the coagulation mechanism. Isoelectric point was observed at around 50 mg Ti/L and 35 mg Al/L. As PTC dosage increased from 15 to 35 mg/L, the zeta potentials of flocs were maintained at around –12.5 to –15 mV, which indicated that sweep flocculation was the main mechanism of coagulation. Further increase of the PTC dosage was accompanied by the increase of both floc zeta potential and the removal of organic matter. Charge neutralization, gradually, came to be the dominant mechanism. Results indicated that, in PTC case, the organic matters (negatively charged) were more likely to be removed by their charge neutralization with positively charged hydrolysates of PTC. The zeta potential of PAC flocs was higher than that of PTC with stronger charge neutralization ability, but resulting in the lower coagulation efficiency. This indicated that, besides charge neutralization, sweep flocculation capability of the hydrolysates of coagulants played a significant role in the removal of pollutants. Some tetravalent cationic hydrolysates formed by PTC were presumably able to interact with more organic compounds

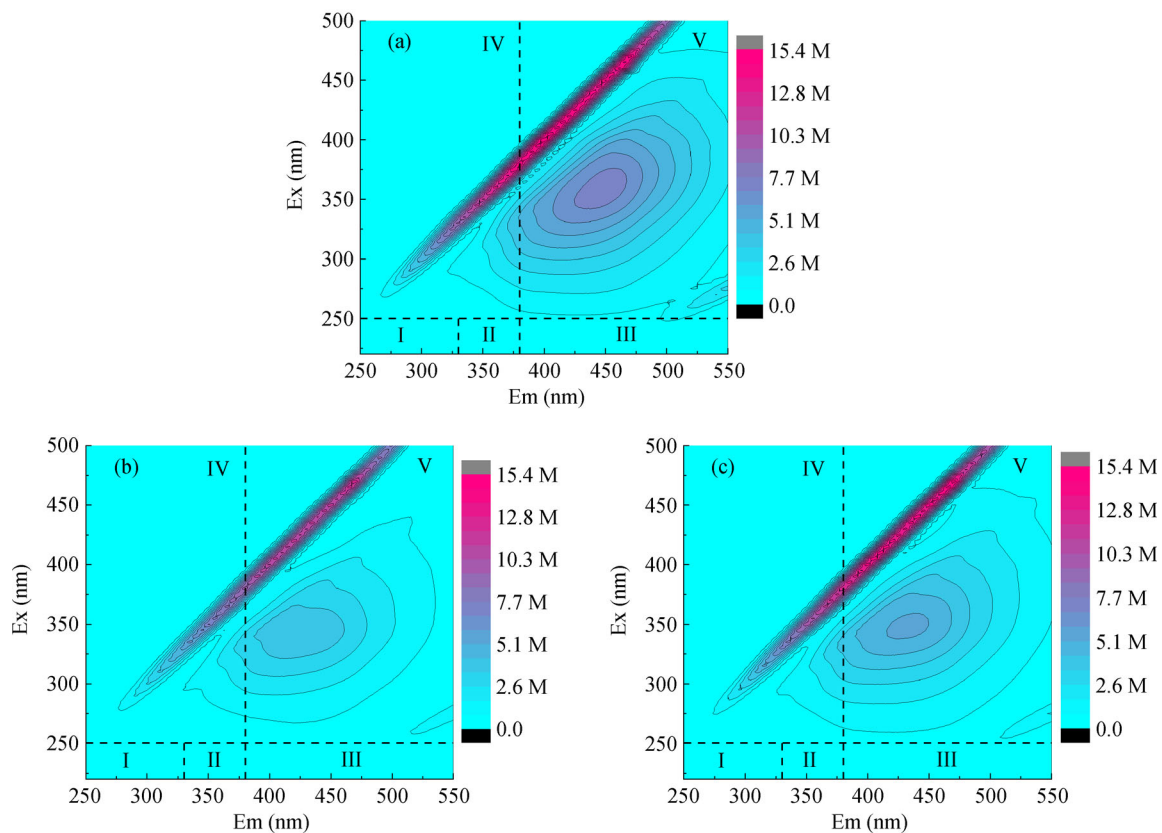


Fig. 2 Three-dimensional excitation emission fluorescence spectra of (a) raw water, (b) the PTC coagulated effluent, and (c) the PAC coagulated effluent (optimum dosage of 50 mg Ti/L and 40 mg Al/L were selected for PTC and PAC coagulation, respectively).

to form large and strong flocs (Zhao and Li, 2019). These findings indicate the superiority of PTC to PAC probably due to both the capability of strong charge neutralization and sweep flocculation. Strong sweep flocculation capability of the PTC hydrolysates was the main reason for its superior removal of organic matter at high dosages.

3.2 Ceramic membrane vs. polymeric membrane filtration

3.2.1 Permeate flux and effluent quality

Ceramic and polymeric membrane (PVDF) were comparatively studied in terms of permeate flux and effluent quality (Fig. 3). According to the experimental results, the filtrate after ceramic membrane filtration had comparable quality as that after PVDF membrane filtration. Low flux (43 L/(m²·h) around) and low DOC removal efficiency (33.0% around) were observed in the direct filtration of RW by ceramic and organic membranes. In contrast, the combined process of coagulation and membrane filtration yielded more satisfactory results. Both ceramic and PVDF membrane filtration produced the filtrate with a DOC removal of 78.0% around, 45.0% higher than that of direct filtration of RW. And the effluent turbidity was below 0.4 NTU, satisfying the general requirements of the water

purification standards. In summary, the PTC pre-coagulation followed by membrane filtration could deliver high-quality filtrate.

As shown in Fig. 3(a), the fluxes during ceramic and PVDF membrane filtration without coagulation exhibited a rapid decline (0–20 min), followed by a plateau with a relatively low value in the early stage, implying that severe fouling behaviour during the early stage of filtration. This fouling contributed to the fact that RW, without coagulation, contained many colloidal particles and macromolecular organic matter. In contrast, pretreatment with coagulants efficiently removed colloidal particles and organic pollutants. As a result, the fluxes after coagulation pretreatment decreased slightly and remained high throughout the filtration process, especially during the ceramic membrane filtration process. The ceramic membrane exhibited an apparent advantage over the polymeric membrane for the PTC coagulated effluent filtration, resulting in high flux up to 600 L/(m²·h) after 10 h of filtration, more than 10-fold higher than that in the case of the polymeric membrane (Fig. 3(a)). Long-term operation of the ceramic membrane filtration (up to 24 h) was further conducted in the lab, with the results being shown in Fig. S2(a). Results show that the ceramic membrane still maintained a relatively high and stable flux of

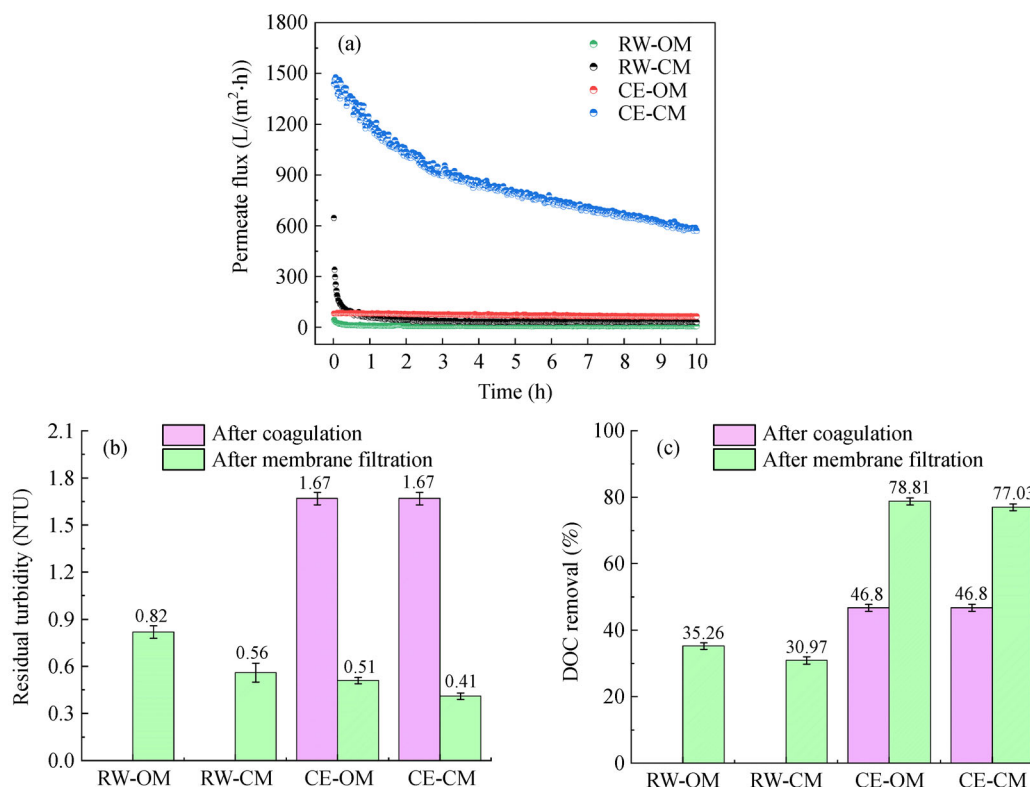


Fig. 3 Comparison of effluent quality and permeate flux between organic membrane and ceramic membrane after coagulation/membrane filtration: (a) permeate flux, (b) residual turbidity, and (c) removal of dissolved organic carbon (DOC) (PTC as coagulant with dosage of 50 mg/L; RW-OM: raw water filtration by organic membrane; RW-CM: raw water filtration by ceramic membrane; CE-OM: filtration of coagulated effluent by organic membrane; CE-CM: filtration of coagulated effluent by ceramic membrane).

400 L/(m²·h) in the 24 h filtration process. The charge on the surface of ceramic membrane may be one of the factors affecting the results. According to the literatures, alumina membranes are positively charged for pH < 8 (Zhao et al., 2021). Therefore, the alumina membrane rejected with the flocs when filtrating the PTC coagulation wastewater (50 mg Ti/L), so as to reduce the membrane fouling and obtain stable and relatively high flux. High-permeate flux and high-quality filtrate through ceramic membrane filtration could enhance the applicability of these membranes in water treatment.

3.2.2 Model analysis of membrane fouling

Mathematical simulation formulas are commonly used to characterize the fouling mechanisms of membrane fouling. Ceramic membrane was just recently developed material for water and wastewater filtration, and hence, reports on the investigation and characterization of ceramic membrane fouling using the mathematical simulation formulas

are limited. Four widely used models (Table 1) of membrane filtration were applied in the present research (Figs. 4 and 5). Herein, the difference in the fouling mechanisms of ceramic membrane and polymeric membrane are discussed.

Ceramic membrane showed a significant advantage over PVDF membrane in terms of permeate flux (Fig. 3(a)). Although, the normalized flux (J/J_0) vs. filtration period (model 1, Fig. 4(a)) presented that ceramic membrane was more inclined to be polluted regardless of the use of a coagulation pretreatment procedure or not. In case of RW, a sharp decline in J/J_0 vs. time in the initial 0.5 h was mainly attributed to the blocking of membrane pores, followed by the gradual formation of a cake layer on the membrane surface, resulting in the slight decline trend of J/J_0 vs. time. The J/J_0 value significantly improved due to the pre-coagulation of PTC.

The same filtration process was simulated by model 2 (Fig. 4(b)), wherein the fouling mechanism was characterized by n value. Then value of 0, 1, 1.5 and 2 represented

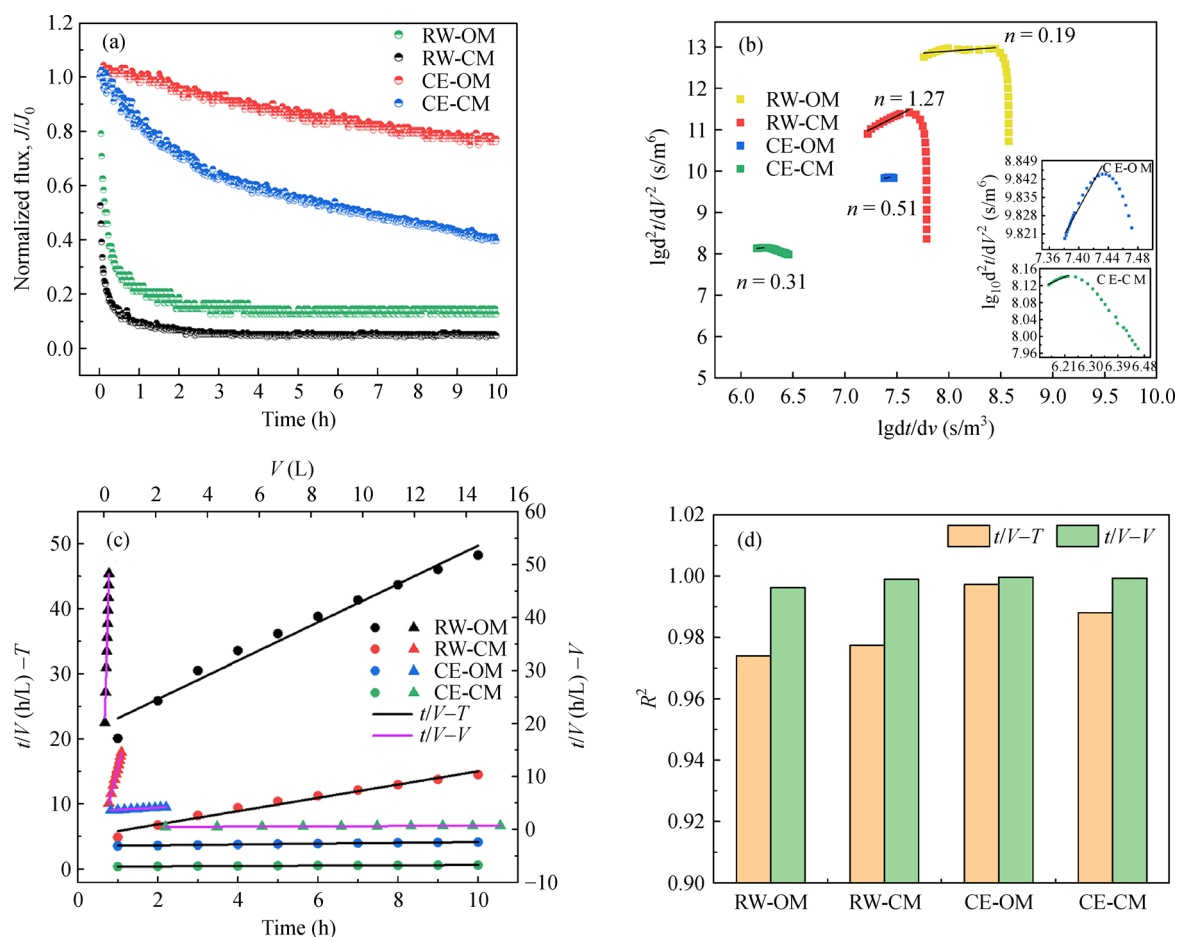


Fig. 4 Comparison of membrane fouling mechanism between organic membrane and ceramic membrane by means of mode 1, 2, and 3: (a) model 1: normalized flux (J/J_0) vs. filtration period; (b) model 2: fitting curves of $\lg d^2 t/dV^2$ vs. $\lg dt/dV$; (c) model 3: fitting curves of t/V vs. T and t/V vs. V ; (d) correlation parameters (R^2) of fitting curves for model 3 (PTC as coagulant with dosage of 50 mg/L; RW-OM: raw water filtration by organic membrane; RW-CM: raw water filtration by ceramic membrane; CE-OM: filtration of coagulated effluent by organic membrane; CE-CM: filtration of coagulated effluent by ceramic membrane).

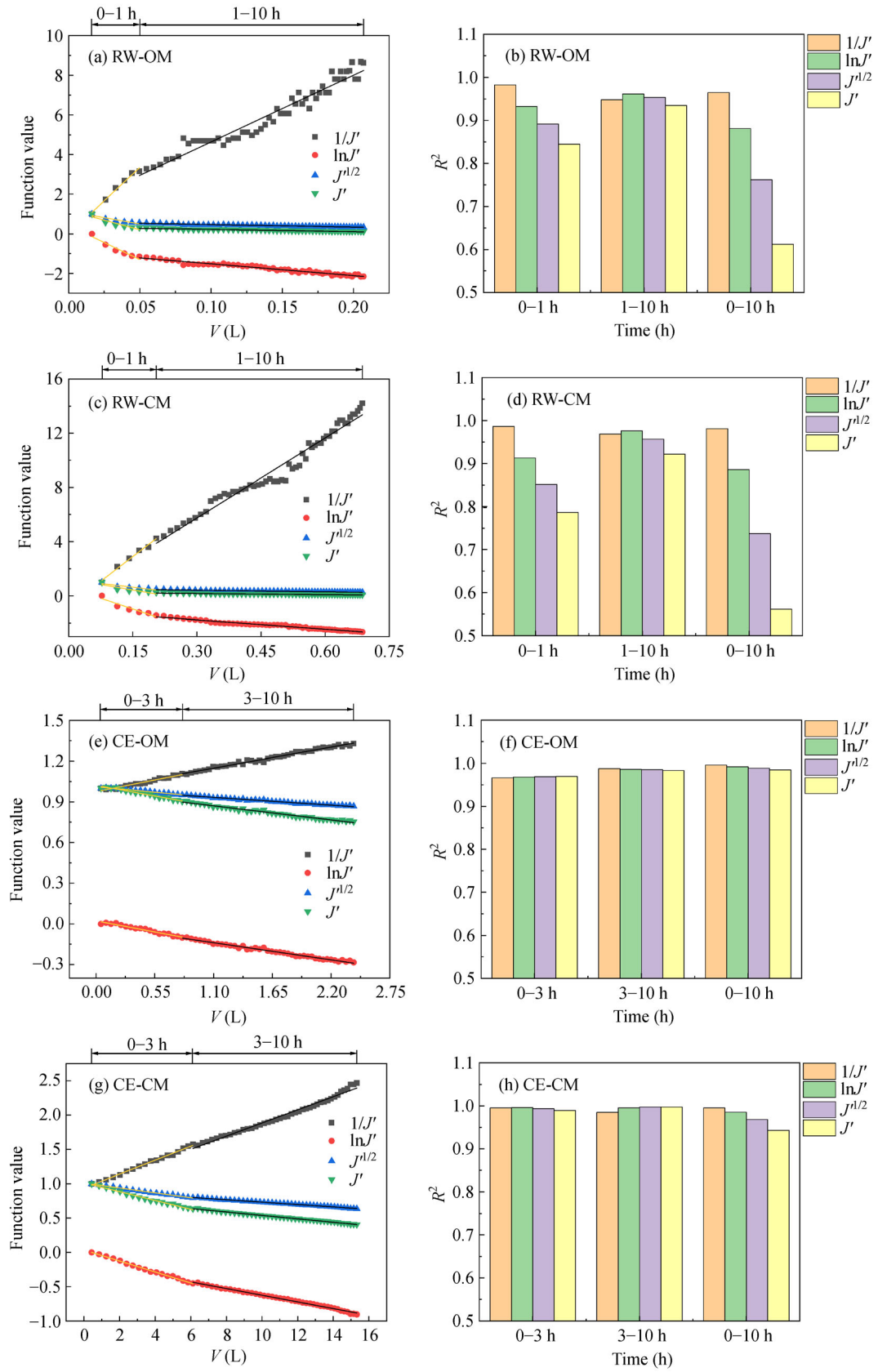


Fig. 5 Fitting curves and correlation parameters (R^2) of model 4 ($1/J'$ vs. V , $\ln J'$ vs. V , $J^{1/2}$ vs. V , and J' vs. V) for four systems at different time segments: (a and b) RW-OM: raw water filtration by organic membrane; (c and d) RW-CM: raw water filtration by ceramic membrane; (e and f) CE-OM: filtration of coagulated effluent by organic membrane; (g and h) CE-CM: filtration of coagulated effluent by ceramic membrane. (PTC as coagulant with dosage of 50 mg/L).

the fouling mechanisms of cake filtration, intermediate blocking, standard filtration and complete blocking, respectively (detailed information refers to Table 1). The n values for RW-OM, RW-CM, CE-OM, and CE-CM were 0.19, 1.27, 0.51, and 0.31, respectively. The incomplete match of these n values to those in model 2 meant that several fouling mechanisms might exist simultaneously in each filtration case. For the filtration of RW, a distinct difference was observed in between ceramic and PVDF membrane, with n values of 0.19 and 1.27, respectively. This difference indicated that the primary fouling mechanism of the ceramic membrane was more likely to be the intermediate blocking and standard blocking, wherein the particles may enter the membrane pores to reduce the membrane pore size. However, for PVDF filtration of RW, the particles were inclined to accumulate on membrane surface to form dense cake layer. This might be the reason why a lower value of J/J_0 was found in the case of ceramic membrane filtration of RW compared to the PVDF (Fig. 4(a)). For both cases of CE-OM and CE-CM, it was speculated that floc and organic matter were deposited on the membrane surface to form permeable cake layer, leading to the gradual decrease in the J/J_0 value vs. filtration period. It was further confirmed by the SEM images presented in Figs. S3 and S4. These showed that both CM and OM were covered by a cake layer formed by flocs, while the cake layer existed on the ceramic membrane surface was much looser. However, according to the results of J/J_0 , CM showed more severe membrane fouling, which might depend on the anti-fouling property of the ceramic membrane. According to Fig. S2(b), only 50% of the flux recovery rate (FRR) was observed, which meant CM has poor anti-fouling properties. In addition, the result of the irreversible flux decline ratio (DR_{ir}) > the reversible flux decline ratio (DR_r) indicated that irreversible flux decay accounts for the majority of flux decays in CM, and irreversible flux could be attributed to contaminants blocking the pores of the ceramic membrane.

The t/V change with time or volume is another classical model for membrane fouling analysis (Figs. 4(c) and 4(d)). The t/V vs. time and t/V vs. volume represented standard law filtration and cake filtration, respectively. The correlation coefficients (R^2) were used to indicate the primary fouling mechanism. In all cases, the R^2 values were all higher than 0.96, which indicated that this mathematical model could not distinguish the main fouling mechanism of the membrane, although the R^2 value of the classic cake filtration model was slightly higher than that of the standard law filtration model. The high R^2 values obtained from t/V vs. time or volume may indicate the co-existence of the two fouling mechanisms.

To further understand the mechanism associated with the evolution of membrane fouling mechanism in the filtration process, model 4 was used to fit the filtration data in sections (Fig. 5). The fitting curves of $1/J'$ vs. V , $\ln J'$ vs. V , $J'^{1/2}$ vs. V , and J' vs. V indicated the fouling of cake

filtration, intermediate blocking, standard blocking and complete blocking, respectively. Considering the severe membrane fouling observed during direct filtration of RW, the whole filtration period was divided into two sections with 1 h as the time division point. For the filtration of the coagulated effluent, 3 h was selected as the time-division point. In case of RW-OM and RW-CM, the higher R^2 from the fitting curve of $1/J'$ vs. V in the initial 1 h of filtration indicated that the main fouling of both ceramic and PVDF membranes could be originated from the formation of the cake layer. During the filtration period between 1 and 10 h, four kinds of fouling mechanisms were speculated to co-exist as evidenced by the high (around 0.95) and comparable R^2 values. Complete blocking could occur as a result of particle blocking of the pores on the cake layer surface. However, given the whole filtration period of 10 h, the formation of the cake layer on the membrane surface was the primary factor associated with the fouling of both ceramic and PVDF membranes. By contrast, in the cases of CE-OM and CE-CM, all the R^2 values simulated from the four mathematical formulas were higher than 0.94, regardless of 0–3 h, 3–10 h, and 0–10 h sections. Thus, the predominant fouling mechanism during the CE-OM and CE-CM filtration could not be clearly defined from model 4.

In summary, the change in J/J_0 value was an effective pathway to elucidate the ceramic membrane's fouling mechanism, with the results showing its apparent difference from the PVDF membrane. The fitting lines from model 2 showed that cake filtration and intermediate blocking/standard blocking were the primary fouling mechanisms for RW-OM and RW-CM, respectively. However, the permeable cake layer mainly contributed to the membrane fouling in both cases of CE-OM and CE-CM. Model 4 was more suitable for the characterization of membrane fouling during RW filtration. Here, the membrane fouling was mainly caused by cake filtration. Model 3 was not recommended in this study, as the dominating fouling mechanism could not be distinguished from the fitting curves.

3.3 PTC vs. PAC pre-coagulation enhanced ceramic membrane filtration

3.3.1 Permeate flux and effluent quality

The PTC coagulant was superior to conventional PAC for organic matter removal (Fig. 1). The use of PTC pretreatment was expected to be highly efficient to obtain both high permeation flux and high-quality filtrate. The comparison between PTC and conventional PAC in terms of filtration performance is detailed in Fig. 6. Herein, the optimized coagulant dosage of 50 mg Ti/L and 40 mg Al/L was selected for PTC and PAC, setting RW as control. Direct filtration of RW was generally unacceptable due to the low removal of organic matter (around 30.0%) and low

permeation flux (around $43 \text{ L}/(\text{m}^2 \cdot \text{h})$). Both PTC and PAC were efficient to improve the filtration performance, especially PTC. After filtration, the removal rates of DOC through PAC or PTC coagulation increased by 27.57% and 46.06%, reaching 58.54% and 77.03%, respectively. The difference in organic matter removal between PTC and PAC was possibly due to the coagulation floc particle size and the pollution layer formation. Due to PTC flocs' larger particle size than that of PAC flocs, PTC flocs tend to be intercepted on the membrane surface to form a large area of pollution layer, thereby blocking the permeability channel of subsequent dissolved organic matter in the early stage of the filtration. For PAC, flocs with smaller particle size could induce more permeability channels on the surface of the membrane, allowing increased penetration of organic matter. The PTC pre-coagulation followed by ceramic membrane filtration produced a high-quality filtrate and showed significantly higher permeate flux than PAC pre-coagulation. For PTC, the initial permeate flux reached $1500 \text{ L}/(\text{m}^2 \cdot \text{h})$, followed by a gradual decline to around $600 \text{ L}/(\text{m}^2 \cdot \text{h})$ in 10 h of filtration, which was more than 3-fold higher than that observed for PAC. Regardless of the pre-coagulation method, the filtration of wastewater using ceramic

membrane was highly-effective for decreasing the turbidity, with the residual turbidity range of 0.41–0.56 NTU, which could satisfy the basic requirement effluent standards.

Coagulant dosage is always a key parameter that influences both coagulation performance and the follow-up membrane filtration process. An insufficient or excessive coagulant dosage could cause serious membrane fouling (Lee et al., 2009). Figure S5 shows the influence of PTC dosage on the performance of ceramic membrane filtration in terms of both filtrate quality and filtration flux. In all cases, following PTC coagulation, ceramic membrane filtration effectively achieved organic matter removal up to 73.0%–79.0% with residual turbidity lower than 1.0 NTU. Moreover, the permeate flux vs. filtration period trend showed obvious differences due to variation of PTC dosage (Fig. S5(a)). A gradual drop in permeate flux was observed with an increasing filtration period in all the cases. The permeate flux followed the order of $50 \text{ mg Ti/L} > 55 \text{ mg Ti/L} > 35 \text{ mg Ti/L}$, which was consistent with the DOC removal rate by PTC of 50 mg Ti/L (46.8%), 55 mg Ti/L (39.9%), and 35 mg Ti/L (35.0%). This sequence indicated that the quality of the effluent after PTC coagulation positively correlated with the flux of ceramic membrane filtration.

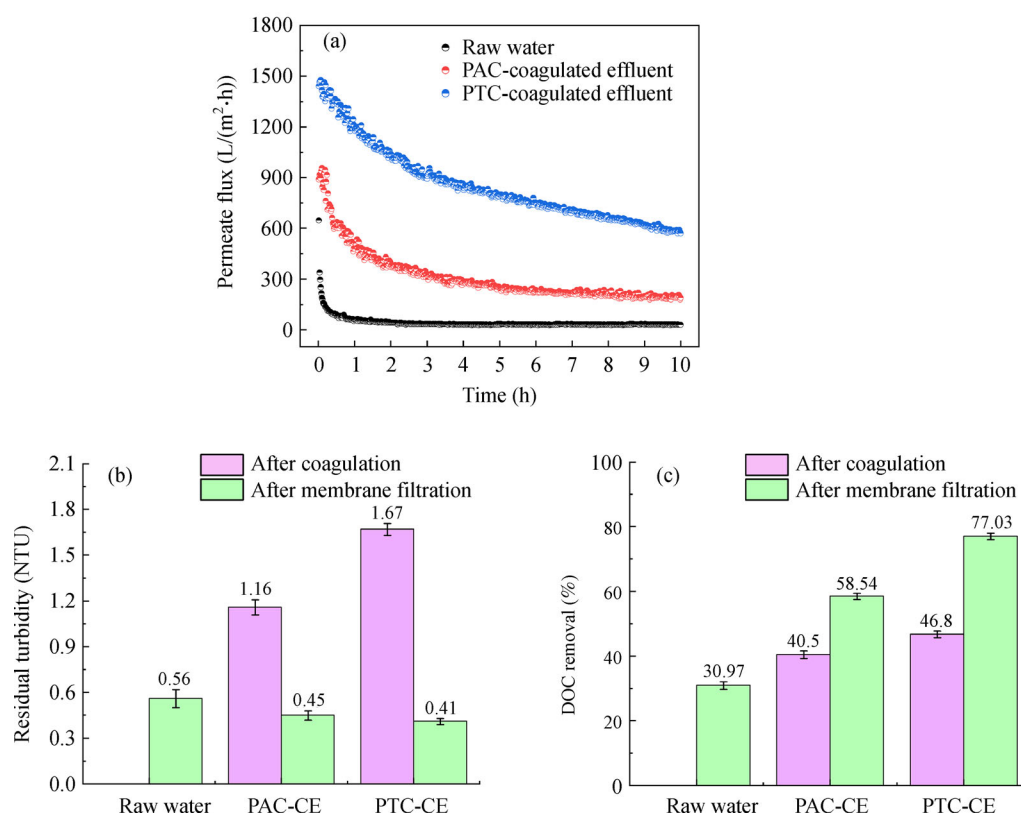


Fig. 6 Comparison of effluent quality after coagulation/ceramic membrane filtration: (a) permeate flux, (b) residual turbidity, and (c) removal of dissolved organic carbon (DOC) (optimum dosage of 50 mg Ti/L and 40 mg Al/L were selected for PTC and PAC coagulation, respectively).

3.3.2 Model analysis of membrane fouling

Four models were utilized to simulate the fouling mechanisms of the ceramic membrane under pre-coagulation of PTC or PAC (Figs. 7 and 8). In addition, the effect of PTC dosage on membrane fouling mechanism was further studied (Figs. S6 and S7).

According to Fig. 7(a), the slowest decline and the highest value of the normalized flux (J/J_0) was observed in PTC case, representing that the lightest membrane fouling occurred in PTC case. To clarify the detailed mechanism of ceramic membrane fouling, $\lg d^2t/dV^2$ vs. $\lg dt/dV$ (model 2) was calculated (Fig. 7(b)), with n values of 1.27, 1.58 and 0.31, respectively, for raw water, PAC₄₀-CE and PTC₅₀-CE. The values of exponent n were not entirely equal for Hermia's model, which indicated that multiple mechanisms caused membrane fouling. The dominant fouling mechanism was the one that represented by the value of n close to Hermia's model. The n value of 1.27 indicated the potential fouling of ceramic membrane attributed to intermediate or standard blocking (Table 1) during the

raw water filtration. The PTC pre-coagulation was an effective strategy to change the fouling mechanism of the ceramic membrane to cake filtration as evidenced by the significant drop of n value to 0.31. A significant difference in the fouling mechanism was observed in PAC case from that of PTC. The blocking of the membrane pores mainly caused the fouling of the ceramic membrane in the PAC case by particles (n values of 1.58). In addition, it was remarkable that the characteristic curves had a negative slope ($n < 0$), which can be expounded by the speed of descending for the dJ/dt and J (Eq. (3)). Owing to the faster decrease of the dJ/dt than J , d^2t/dV^2 and $\lg d^2t/dV^2$ decreased simultaneously. Moreover, the appearance of a negative slope after the peak value meant that the filtration mechanism changed to cake filtration (Lee et al., 2013).

Titanium-based coagulation was previously known to produce large flocs with good sedimentation capability. However, the blocking of the membrane pores in PAC case was probably due to the small floc size. The particle size distribution (PSD) (Fig. 9) further validated this speculation. The PSD of PAC-coagulated effluent was mainly

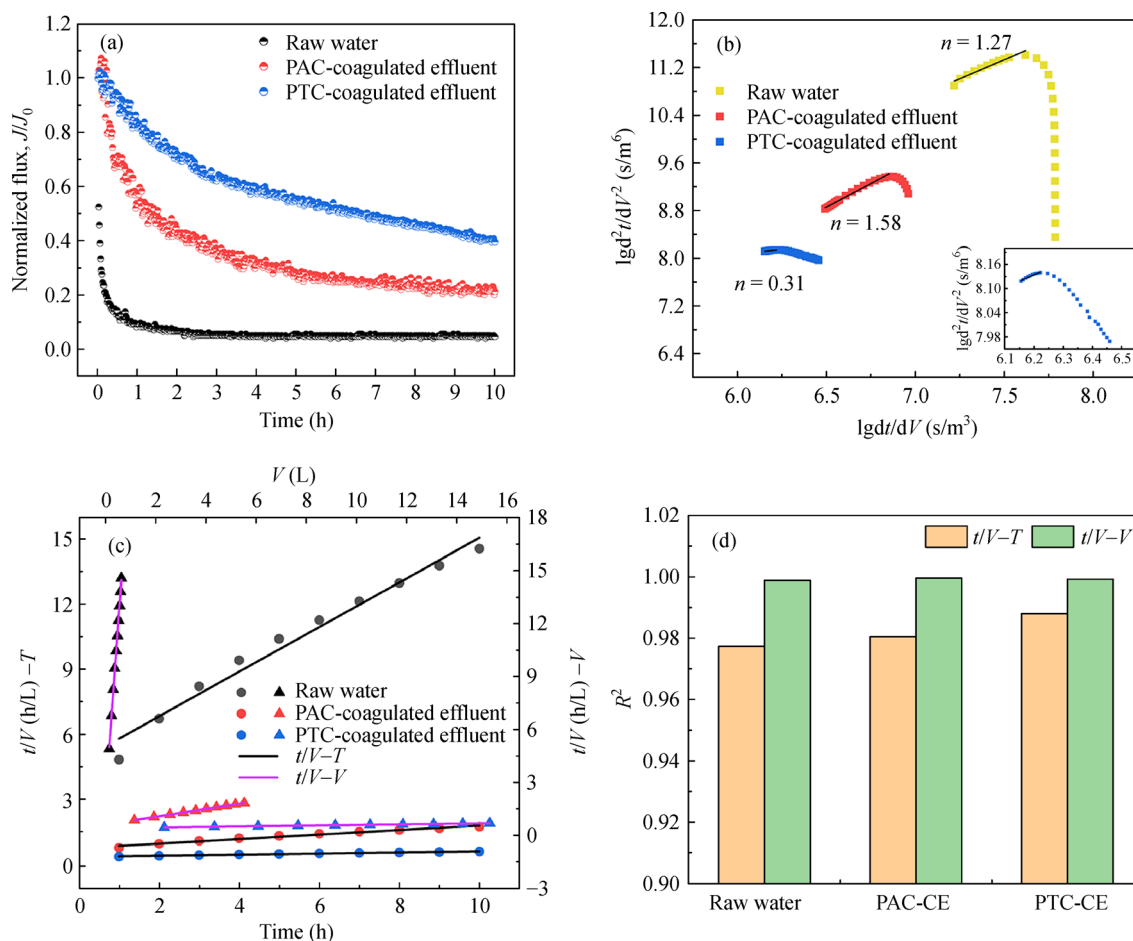


Fig. 7 Comparison of membrane fouling mechanism between raw water, PTC coagulated effluent (CE), and PAC coagulated effluent by means of mode 1, 2, and 3: (a) model 1: normalized flux (J/J_0) vs. filtration period; (b) model 2: fitting curves of $\lg d^2t/dV^2$ vs. $\lg dt/dV$; (c) model 3: fitting curves of t/V vs. T and t/V vs. V ; (d) correlation parameters (R^2) of fitting curves for model 3 (optimum dosage of 50 mg Ti/L and 40 mg Al/L were selected for PTC and PAC coagulation, respectively).

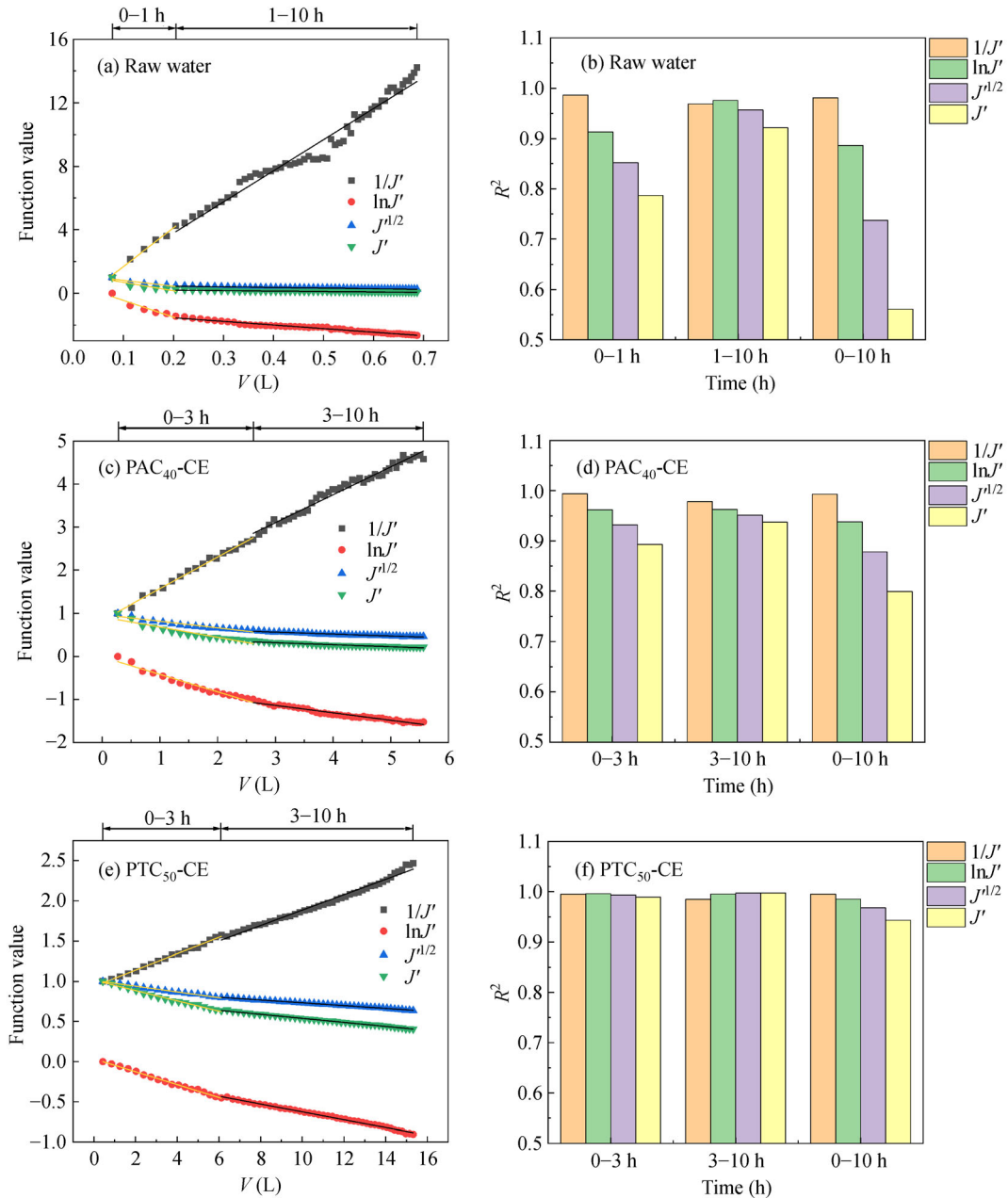


Fig. 8 Fitting curves and correlation parameters (R^2) of model 4 ($1/J'$ vs. V , $\ln J'$ vs. V , $J'^{1/2}$ vs. V and J' vs. V) for raw water, PTC coagulated effluent (CE), and PAC coagulated effluent: ceramic membrane: (a and b) raw water; (c and d) PAC coagulated effluent; (e and f) PTC coagulated effluent (optimum dosage of 50 mg Ti/L and 40 mg Al/L were selected for PTC and PAC coagulation, respectively).

distributed in the range of 10–62 μm , whereas that of PTC-coagulated effluent was 25–255 μm . Thus, the larger flocs in PTC-coagulated effluent resulted in the rapid formation of the cake layer on the membrane surface, and the dissolved organic matter not removed by coagulation was removed by the cake layer again during filtration. On the contrary, PAC-coagulated effluent may contain many small-sized residual flocs and micro-organic pollutants, which tended to adsorb into the membrane pores to form pore blocking. As observed from the SEM micrographs

(Fig. S4), there were more pores in the cake layer on the fouled membrane surface in PAC. These pores enhanced the penetration of the tiny organic matter into the membrane and resulted in the blockage of the membrane pores and low DOC removal. The adsorption of flocs with small particle size on the membrane surface or even in the membrane pore led to the double resistance of membrane pores blockage and cake layer blockage in the filtration of PAC-coagulated effluent.

By means of the analysis of Model 3 (Figs. 7(c) and

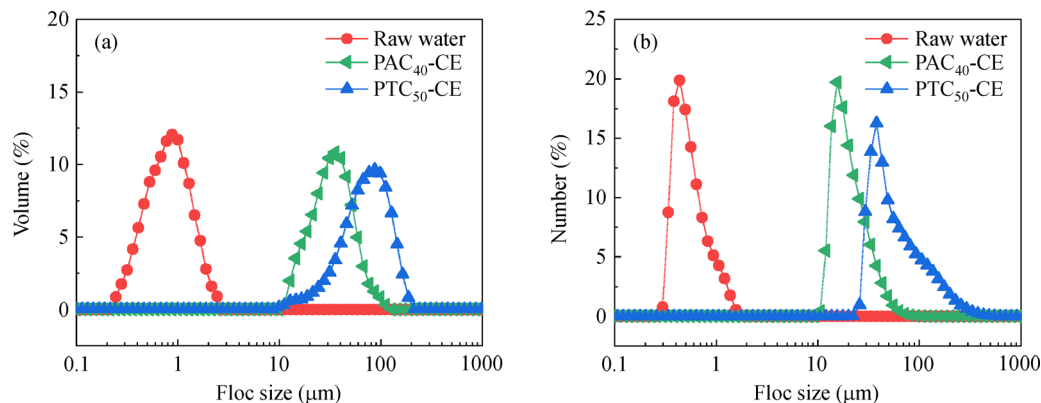


Fig. 9 Volume-based (a) and number-based (b) floc size distribution of raw water, PAC coagulated effluent, and PTC coagulated effluent under optimum dosage (optimum dosage of 50 mg Ti/L and 40 mg Al/L were selected for PTC and PAC coagulation, respectively).

7(d)) and Model 4 (Fig. 8), it was consistently concluded that the membrane fouling process under the three filter inlet conditions was all dominated by filter cake layer blocking. All the R^2 values obtained from model 3 were >0.98 , indicating that this model could not identify the primary fouling mechanism. Regarding model 4, the main difference in the R^2 values appeared in the time range of 0–3 h. The cake layer blocked the ceramic membrane when raw water and PAC-coagulated effluent were utilized as the influent of filtration. On the other hand, while the ceramic membrane was polluted by several common pollution mechanisms when PTC coagulation effluent was used as the influent. Similar R^2 values were obtained during 3–10 h of filtration. The fouling of ceramic membranes in the whole filtration period was often the one that got the most attention. In both PAC-CE and PTC-CE filtration in 10 h, the R^2 values from the simulation followed the order of $1/J$ vs. $V > \ln J$ vs. $V > J^{1/2}$ vs. $V > J$ vs. V , indicating that the most probable fouling mechanism of the ceramic membrane was cake filtration.

In summary, model 1 and model 2 (Table 1) mentioned above were effective methodologies to identify the difference between PAC and PTC cases regarding the fouling mechanisms of ceramic membrane. The ceramic membrane was more likely to be polluted by the cake layer in PTC case. On the other hand, while using PAC, the blocking of ceramic membrane pores was also a significant cause of membrane fouling. The results were consistent with those obtained from the simulation of the J/J_0 vs. filtration period (Fig. 7(a)). For model 3, the fouling mechanism of standard law filtration and cake filtration could not be distinguished from each other. Moreover, for model 4, a segmented simulation was required to differentiate the fouling mechanisms. Additionally, the quality of the influent had a significant influence on the fouling mechanism of the ceramic membrane. The inclusion of fouling analysis would be beneficial to select the high-efficiency coagulant for water and wastewater treatment.

3.4 Macroeconomic efficiency analysis

Coagulation-filtration combined process is widely used for the treatment of drinking water and advanced water treatment due to its advantages of good treatment effect, low cost and simple operation. The type of coagulant and the choice of membrane material for filtration determine the performance of the combined process. In recent years, it has been reported that titanium-based coagulants show better coagulation performance than traditional aluminum-based and iron-based coagulants (Zhao et al., 2015). What's more, the sludge after titanium-based coagulation could be recycled to obtain valuable nano titanium dioxide (Chi et al., 2019). Practical use of titanium-based coagulants will make great contribution to water purification and resource utilization. Price of the titanium-based coagulants, such as $TiCl_4$ was about 1000 Yuan RMB/ton, comparable to that of the conventional PAC. Recycling of the titanium-coagulated sludge to produce functional TiO_2 was not only economically benefit, but also environmentally available to solve the problem of sludge disposal.

As far as filtration is concerned, at present, polymeric membranes are widely utilized, while ceramic membranes are rarely used because of its high cost. However, ceramic membrane has received significant attention due to their high filtration flux, fouling resistance propensity, and chemical- and mechanical- resistance. Nowadays, although the price of ceramic membrane (2200 to 4500 Yuan RMB/m²) is higher than polymeric membrane (95 to 500 Yuan RMB/m²), they have a longer service life (about 20 years), while the service life of polymeric membranes is only about 3–5 years (Asif and Zhang, 2021). Long service time is a compensation for their high price. Moreover, the durability and fouling resistance make long-term filtration of ceramic membrane a great possibility, which avoid frequent replacement of membranes and therefore save manpower and financial resources. With the development of ceramic technology, price of ceramic membrane is going down, which makes the cost of polymeric membrane and

ceramic membrane competitive. To sum up, the titanium-based pre-coagulation was superior to the conventional aluminum-based and iron-based coagulation, resulting in the coagulated effluent with higher quality (Fig. 1). The follow-up filtration of the effluent with ceramic membrane could produce 1) filtrate with improved quality, and 2) significant higher flux of permeation. Not only the performance of coagulation, but also the cross-flow performance of ceramic membrane could be greatly improved by titanium-based salts.

4 Conclusions

This study investigated the enhanced cross-flow performance of ceramic membrane by PTC pre-coagulation. The performance of PAC was studied for comparison. The PTC showed a significant advantage over PAC, resulting in about 20% higher organic matter removal. The follow-on filtration of the PTC-coagulated effluent with ceramic membrane produced a filtrate with improved quality (about 78.0% removal of DOC) and a high flux of around 600 L/(m²·h). By contrast, the PVDF membrane filtration could obtain comparable DOC removal (about 77.0%), but with a low filtration flux of ca. 60 L/(m²·h) only. Four mathematical models were involved in simulating the fouling mechanisms of ceramic membranes. In PTC case, the trend of J/J_0 vs. time showed the slower and less fouling of the ceramic membrane. At the same time, the simulation of the classical Hermia's model indicated the main fouling mechanism of cake filtration. The t/V vs. t and t/V vs. V (model 3) was not suggested for fouling characterization of the ceramic membrane, with the R^2 values > 0.98 in all the cases. A segmented simulation was required to distinguish the difference of fouling mechanisms between PTC and PAC cases using linear classical Hermia's model.

Acknowledgements This work was supported by the National Natural Science Foundation of China (Grant No. 51978311), Taishan Scholars Young Experts Program (China) (No. tsqn202103080), and Shandong Provincial Natural Science Foundation, China (No. ZR2019BEE044).

Electronic Supplementary Material Supplementary material is available in the online version of this article at <https://doi.org/10.1007/s11783-022-1531-x> and is accessible for authorized users.

References

- Asif M B, Zhang Z (2021). Ceramic membrane technology for water and wastewater treatment: A critical review of performance, full-scale applications, membrane fouling and prospects. *Chemical Engineering Journal*, 418: 129481
- Chekli L, Eripret C, Park S H, Tabatabai S A A, Vronska O, Tamburic B, Kim J H, Shon H K (2017). Coagulation performance and floc characteristics of polytitanium tetrachloride (PTC) compared with titanium tetrachloride (TiCl₄) and ferric chloride (FeCl₃) in algal turbid water. *Separation and Purification Technology*, 175: 99–106
- Chi Y, Tian C, Li H, Zhao Y (2019). Polymerized titanium salts for algae-laden surface water treatment and the algae-rich sludge recycle toward chromium and phenol degradation from aqueous solution. *ACS Sustainable Chemistry & Engineering*, 7(15): 12964–12972
- Galloux J, Chekli L, Phuntsho S, Tijing L D, Jeong S, Zhao Y X, Gao B Y, Park S H, Shon H K (2015). Coagulation performance and floc characteristics of polytitanium tetrachloride and titanium tetrachloride compared with ferric chloride for coal mining wastewater treatment. *Separation and Purification Technology*, 152: 94–100
- Ghalami Choobar B, Alaei Shahmirzadi M A, Kargari A, Manouchehri M (2019). Fouling mechanism identification and analysis in microfiltration of laundry wastewater. *Journal of Environmental Chemical Engineering*, 7(2): 103030
- He C, Vidic R D (2016). Application of microfiltration for the treatment of Marcellus Shale flowback water: Influence of floc breakage on membrane fouling. *Journal of Membrane Science*, 510: 348–354
- Hou L, Wang Z, Song P (2017). A precise combined complete blocking and cake filtration model for describing the flux variation in membrane filtration process with BSA solution. *Journal of Membrane Science*, 542: 186–194
- Huang H, Young T A, Jacangelo J G (2008). Unified membrane fouling index for low pressure membrane filtration of natural waters: principles and methodology. *Environmental Science & Technology*, 42(3): 714–720
- Jia H, Feng F, Wang J, Ngo H H, Guo W, Zhang H (2019). On line monitoring local fouling behavior of membrane filtration process by in situ hydrodynamic and electrical measurements. *Journal of Membrane Science*, 589: 117245
- Lee B B, Choo K H, Chang D, Choi S J (2009). Optimizing the coagulant dose to control membrane fouling in combined coagulation/ultrafiltration systems for textile wastewater reclamation. *Chemical Engineering Journal*, 155(1–2): 101–107
- Lee S J, Dilaver M, Park P K, Kim J H (2013). Comparative analysis of fouling characteristics of ceramic and polymeric microfiltration membranes using filtration models. *Journal of Membrane Science*, 432: 97–105
- Li W, Chen M, Zhong Z, Zhou M, Xing W (2020). Hydroxyl radical intensified Cu₂O NPs/H₂O₂ process in ceramic membrane reactor for degradation on DMAc wastewater from polymeric membrane manufacturer. *Frontiers of Environmental Science & Engineering*, 14(6): 102
- Li W, Hang F, Li K, Lei F (2019). Development and application of combined models of membrane fouling for the ultrafiltration of limed sugarcane juice. *Sugar Tech*, 21(3): 524–526
- Ma N, Zhang Y, Quan X, Fan X, Zhao H (2010). Performing a microfiltration integrated with photocatalysis using an Ag-TiO₂/HAP/Al₂O₃ composite membrane for water treatment: Evaluating effectiveness for humic acid removal and anti-fouling properties. *Water Research*, 44(20): 6104–6114
- Park J, Jeong K, Baek S, Park S, Ligaray M, Chong T H, Cho K H (2019). Modeling of NF/RO membrane fouling and flux decline using real-time observations. *Journal of Membrane Science*, 576: 66–77
- Shen Y, Zhao W, Xiao K, Huang X (2010). A systematic insight into

- fouling propensity of soluble microbial products in membrane bioreactors based on hydrophobic interaction and size exclusion. *Journal of Membrane Science*, 346(1): 187–193
- Shon H K, Phuntsho S, Vigneswaran S, Kandasamy J, Nghiem L D, Kim G J, Kim J B, Kim J H (2010). Preparation of titanium dioxide nanoparticles from electrocoagulated sludge using sacrificial titanium electrodes. *Environmental Science & Technology*, 44(14): 5553–5557
- Visvanathan C, Ben aim R (1989). Studies on colloidal membrane fouling mechanisms in crossflow microfiltration. *Journal of Membrane Science*, 45(1–2): 3–15
- Wang H, Park M, Liang H, Wu S, Lopez I J, Ji W, Li G, Snyder S A (2017). Reducing ultrafiltration membrane fouling during potable water reuse using pre-ozonation. *Water Research*, 125: 42–51
- Wei S, Du L, Chen S, Yu H T, Quan X (2021). Electro-assisted CNTs/ceramic flat sheet ultrafiltration membrane for enhanced antifouling and separation performance. *Frontiers of Environmental Science & Engineering*, 15(1): 11
- Werber J R, Osuji C O, Elimelech M (2016). Materials for next-generation desalination and water purification membranes. *Nature Reviews. Materials*, 1(5): 16018
- Xu Z, Wu T, Shi J, Teng K, Wang W, Ma M, Li J, Qian X, Li C, Fan J (2016). Photocatalytic antifouling PVDF ultrafiltration membranes based on synergy of graphene oxide and TiO₂ for water treatment. *Journal of Membrane Science*, 520: 281–293
- Yang T, Xiong H, Liu F, Yang Q, Xu B, Zhan C (2019). Effect of UV/TiO₂ pretreatment on fouling alleviation and mechanisms of fouling development in a cross-flow filtration process using a ceramic UF membrane. *Chemical Engineering Journal*, 358: 1583–1593
- Zhan M, Kim Y, Lim J, Hong S (2021). Application of fouling index for forward osmosis hybrid system: A pilot demonstration. *Journal of Membrane Science*, 617: 118624
- Zhang B, Mao X, Tang X, Tang H, Zhang B, Shen Y, Shi W (2022). Pre-coagulation for membrane fouling mitigation in an aerobic granular sludge membrane bioreactor: A comparative study of modified microbial and organic flocculants. *Journal of Membrane Science*, 644: 120129
- Zhao C, Yu X, Da X, Qiu M, Chen X, Fan Y (2021). Fabrication of a charged PDA/PEI/Al₂O₃ composite nanofiltration membrane for desalination at high temperatures. *Separation and Purification Technology*, 263: 118388
- Zhao Y X, Gao B Y, Qi Q B, Wang Y, Phuntsho S, Kim J H, Yue Q Y, Li Q, Shon H K (2013). Cationic polyacrylamide as coagulant aid with titanium tetrachloride for low molecule organic matter removal. *Journal of Hazardous Materials*, 258–259: 84–92
- Zhao Y X, Gao B Y, Zhang G Z, Qi Q B, Wang Y, Phuntsho S, Kim J H, Shon H K, Yue Q Y, Li Q (2014). Coagulation and sludge recovery using titanium tetrachloride as coagulant for real water treatment: A comparison against traditional aluminum and iron salts. *Separation and Purification Technology*, 130: 19–27
- Zhao Y X, Li X Y (2019). Polymerized titanium salts for municipal wastewater preliminary treatment followed by further purification via crossflow filtration for water reuse. *Separation and Purification Technology*, 211: 207–217
- Zhao Y X, Phuntsho S, Gao B Y, Yang Y Z, Kim J H, Shon H K (2015). Comparison of a novel polytitanium chloride coagulant with polyaluminium chloride: Coagulation performance and floc characteristics. *Journal of Environmental Management*, 147: 194–202
- Zhao Y X, Sun Y Y, Gao B Y, Wang Y, Yang Y Z (2017). Inhibition of disinfection by-product formation in silver nanoparticle-humic acid water treatment. *Separation and Purification Technology*, 184: 158–167